CHANDRA OBSERVATIONS OF VARIABLE EMBEDDED X-RAY SOURCES IN ORION. PAPER I: RESOLVING THE ORION TRAPEZIUM

N.S. SCHULZ[1], C. CANIZARES[1], D. HUENEMOERDER[1], J.H. KASTNER[2], S.C. TAYLOR[1], E.J. BERGSTROM[2]

accepted for publication in The Astrophysical Main Journal

ABSTRACT

We used the High Energy Transmission Grating Spectrometer (HETGS) onboard the Chandra X-ray Observatory to perform two observations, separated by three weeks, of the Orion Trapezium region. The zeroth order images on the Advanced CCD Imaging Spectrometer (ACIS) provide spatial resolution of 0.5" and moderate energy resolution. Within a 160"x140" region around the Orion Trapezium we resolve 111 X-ray sources with luminosities between 7×10^{28} erg s^{-1} and 2×10^{32} erg s^{-1}. We do not detect any diffuse emission. All but six sources are identified. From spectral fits of the three brightest stars in the Trapezium we determine the line of sight column density to be $N_H = 1.93 \pm 0.29 \times 10^{21}$ cm^{-2}. Many sources appear much more heavily absorbed, with N_H in the range of 10^{22} to 10^{23} cm^{-2}. A large fraction of sources also show excursions in luminosity by more than a factor 5 on timescales >50 ks; many are only detected in one of the observations.

The main objective of this paper is to study the Orion Trapezium and its close vicinity. All five Trapezium stars are bright in X-rays, with θ^1 Ori C accounting for about 60% of the total luminosity of the Trapezium. The CCD spectra of the three very early type members can be fit with a two-temperature thermal spectrum with a soft component of kT ~ 0.8 keV and a hard component of kT ~ 2 to 3 keV. θ^1 Ori B is an order of magnitude fainter than θ^1 Ori E and shows only a hard spectrum of kT ~ 3 keV. θ^1 Ori D is another order of magnitude fainter than θ^1 Ori B, with only a kT ~ 0.7 keV component. We discuss these results in the context of stellar wind models.

We detect eight additional, mostly variable X-ray sources in the close vicinity of the Trapezium. They are identified with thermal and non-thermal radio sources, as well as infrared and optical stars. Five of these X-rays sources are identified with proplyds and we argue that the X-ray emission originates from class I, II and III protostars at the cores of the proplyds.

Subject headings: stars: clusters — stars: formation — stars: early type — X-rays: stars — techniques: spectroscopic

1. INTRODUCTION

The Trapezium Cluster of the Orion Nebula is one of the best studied star forming regions. At a distance of 440 pc, the Trapezium Cluster is embedded at the near rim of the giant dark molecular cloud L1641, lying just behind the Orion Nebula (NGC 1976). It is the core of the Orion Nebula Cluster (ONC), a loose association of more than 5000 mostly very young (< 1-2 Myr) pre-main sequence stars of a wide range of stellar mass ($\sim 0.1 - 50 \ M_\odot$) within a radius of about 1.3 pc (see Hillenbrand 1997 and references therein). A density of $\sim 5 \times 10^3$ stars per pc^3 within the central 0.1 pc makes the Trapezium Cluster the most dense stellar clustering known in our Galaxy (McCaughrean & Stauffer 1994) with about 3000 $M_\odot$ pc^{-3}.

The Orion Trapezium was discovered by Trumpler (1931) and its main stellar component, θ^1 Ori C, was identified as the main source of excitation of the Orion Nebula. Many observations of the Trapezium have been made at infrared wavelengths, mainly the K- and H-bands at 2.20 μm and 1.65 μm respectively. θ^1 Ori A - E are the brightest stars in the cluster, optically and at infrared wavelengths, and are early type O or B-stars. Three members of the Trapezium are multiple systems, some with separations much smaller than 90 AU (Petr et al. 1986). About 80 % of the stars are younger than 1 Myr with a median age of 3×10^5 yr. The present star formation rate is estimated at $\sim 10^{-4} \ M_\odot$ yr^{-1} (Hillenbrand 1997).

The core of the Orion Nebula is one of the prime areas to observe and study very young stellar objects (YSOs). Laques & Vidal (1979) detected externally illuminated YSOs in the form of compact Hα brightness knots, which are illuminated by the two optically brightest sources, θ^1 Ori C and θ^1 Ori A. Garay et al. 1987 measured free-free radio continua from most of these sources. Many so-called 'proplyd' (externally illuminated protoplanetary disk) candidates have been discovered in the vicinity of the Trapezium (O'Dell et al. 1993), many of which correspond to radio and/or IR sources (Felli et al. 1993; McCaughrean and Stauffer 1994). Bally et al. (1998) studied over 40 proplyds with HST and discussed models for these illuminated YSOs involving a young star at the core with a circumstellar disk embedded in an outer wind shock region, as well as a wind driven tail pointing away from the illuminating star.

Because of its proximity, the Orion Trapezium came under early scrunity in X-rays and it was UHURU, the first X-ray satellite (Giacconi et al. 1971), that discovered X-rays from that region in 1972. The *Einstein* Observatory for the first time observed X-rays identified with main sequence O6 to B5 stars (Cassinelli et al. 1981). These early type stars do not have a stellar corona like late type stars, but exhibit a very hot stellar wind that ionizes its environment. Here X-rays are generally thought to originate from bow shocks surrounding radiatively driven blobs plowing through rarified wind material (Lucy and White 1980). Surprisingly, X-rays from some late-B and early A-type stars were discovered, where neither a corona nor an im-

[1] Center for Space Research, Massachusetts Institute of Technology, Cambridge MA 02139, USA

[2] Chester F. Carlson Center for Imaging Science, Rochester Institute of Technology, Rochester NY 14623, USA

portant stellar wind is thought to exist. The generally favored explanantion for these X-rays is that they originate not from the star itself but from an unresolved, otherwise invisible low-mass companion (Berghöfer and Schmitt 1994). On the other hand the ONC hosts a large sample of late type pre-main sequence (PMS) stars. *Einstein* and *ROSAT* established a large catalog of X-ray sources within an area of 5'x5', of which over 200 objects were identified as PMS stars with spectral types of F to late G (Ku & Chanan 1979, Gagne et al. 1995, Geier et al. 1995). These stars generate X-rays through magnetic activity and a hot corona. It has also been suggested that the Trapezium Cluster itself features a faint diffuse X-ray component from ionized material in between the Trapezium stars (Ku & Chanan 1979).

With the launch of ROSAT in 1990, individual X-ray sources were resolved in the Trapezium (Caillault et al. 1994; Gagne et al. 1995), however the question of a diffuse X-ray component within the Trapezium remained (Geier et al. 1995). The *ASCA* observatory launched in 1993 observed the Orion Trapezium cluster with its until then unprecedented spectral resolving capacity up to 10 keV. The results showed that a high temperature plasma with $kT \sim 2-5$ keV exists in the Trapezium, and 2-temperature thin thermal plasmas are more likely than single temperatures (Yamauchi et al. 1996). This is in agreement with the observations of O-stars with *ASCA* (Corcoran et al. 1994), which obtained spectra of δ Ori and λ Ori characterized by two-temperature models with additional absorption attributed to a warm wind. The hot components had temperatures of $kT \sim$ 0.6 and 2 keV. The *ASCA* observations also did not observe the large flares one expects from late type T Tauri stars, but the spectra showed the existence of a variable hard spectral component associated with the Trapezium.

The physical origin of highly energetic emission from young stars is still uncertain. So far only empirical relationships exist between this emission and stellar age, size and mass of the star, as well as stellar rotation (Feigelson et al. 1993, Kastner et al. 1997). We currently classify evolutionary traces simply by observability in the radio to X-ray band. Class 0 sources are considered to be still deeply embedded and merely gravitationally collapsing cores and the spectral energy distribution peaks in the far-IR/submm range. Class I sources are accreting from a protostellar cloud and are optically obscured. The slope of these spectra is known to rise from near-IR through far-IR. Class II sources or classical T Tauri stars (CTTS) are strongly visible in the optical in the Hα-line but also have a substantial IR excess. Class III sources or weak line T Tauri stars (WTTS) are optically bright with little or no IR excess; see the review by Feigelson & Montmerle (1999) and references therein. *ASCA* recently detected giant X-ray flares with variable hard X-ray emission from YSOs (Kamata et al. 1997, Tsuboi et al. 1998, Yamauchi & Kamimura 1999, Tsuboi et al. 2000). Spectral temperatures ranged from $kT \sim$ 4 - 6 keV, in extreme cases up to > 10 keV. A recent modeling of these X-ray flares from two class I protostars relates this emission to strong magnetic shearing and reconnection between the central star and the sourrounding protostellar accretion disk (Montmerle et al. 2000).

The next steps toward a better understanding of the astrophysical processes underlying high energy emission at early stages of stellar evolution can be made with the Chandra X-ray Observatory. The Orion Nebula Cluster was observed early in the Chandra mission by Garmire et al. 2000, who detected about 1000 resolved X-ray sources, the richest field of sources ever imaged in X-rays. The observation was performed with a wide field of view and therefore was best suitable for studying the overall demographics of the X-ray emission in the whole Orion Nebula Cluster. From the placement of the identified sources in the Hertzsprung-Russell (HR) diagram it was concluded that a large fraction of the cluster members with masses above 1 $M_\odot$ are detected in X-rays, whereas the detection rate decreases rapidly for lower mass stars.

In our observations we focus on a smaller field of view around the Trapezium, which suffers from saturation effects in the Garmire et al. (2000) data. Our objective is to resolve the Orion Trapezium cluster core in X-rays and to perform a detailed spectral analysis on the bright sources as well as to study the variability of the X-ray emission. We present the results from the zero order field analysis in three parts. Paper I gives an overview of these observations but focuses on the X-ray properties of the Orion Trapezium and its very close vicinity within a radius of 15". Paper II (Kastner et al. 2000, in preparation) then discusses identifications within the whole available field of view around the Orion Trapezium with known infrared and radio catalogs as well as with newly obtained IR observations. In paper III (Schulz et al. 2000a, in preparation) we present X-ray spectroscopy on the whole field of view. Schulz et al. (2000) also present high resolution spectroscopy of θ^1 Ori C using the first order spectra of the HETGS.

2. CHANDRA OBSERVATIONS AND DATA ANALYSIS

The Chandra X-ray Observatory (Weisskopf et al. 1996) was launched on the 23rd of July 1999 into a highly eccentric 72 h orbit to allow uninterrupted observations of up to 140 ks. Chandra has an unprecedented spatial resolution of 0.5 arcsec (225 AU at the distance of the Trapezium). Besides its spatial resolving capabilities, Chandra also allows for medium resolution spectroscopy ($E/\Delta E$=6-60) in the 0.1 to 10.0 keV band using the Advanced CCD Imaging Spectrometer (ACIS) and high resolution spectroscopy with $E/\Delta E$ of up to 1200 at 1 keV using gratings. For detailed descriptions of the spectroscopic instruments see Garmire et al. (2000, in preparation), Markert et al. (1994) and Canizares et al. (2000, in preparation).

We obtained two observations of the Trapezium Cluster using the High Resolution Transmission Grating Spectrometer (HETGS), the first on October 31st UT 05:47:21 1999, the second about three weeks later on November 24th UT 05:37:54 1999, for durations of 50 ks and 33 ks, respectively. In this paper we report on data obtained with the CCD camera in the 0th order of the HETGS with the aimpoint on the Orion Trapezium (RA $5^h35^m14.5^s$ and Dec $-5^o23'32''$), which was positioned on the middle of the central back-illuminated CCD device S3 on node 0. This device was unaffected by the degradation of charge transfer inefficiency of the ACIS front illuminated CCDs due to high dosage of particle irradiation early into the mission as reported by Prigozhin et al. (2000). Because the zeroth order image contains roughly 30% of the flux that would be incident on ACIS if HETG were not inserted, it is less susceptible to the effects of photon pileup in the CCDs. There are no apparent image distortions due to pileup, and only the CCD spectrum of the brightest source, θ^1 Ori C, appears to be affected by pileup.

The Chandra X-ray Center (CXC) provided aspect corrected level 1 event lists via standard pipeline processing. We reprocessed these data using the most updated calibration data products and ACIS-S detector to sky transformations available to us. We also removed all events that resulted from either bad pixels or columns as well as from flaring background events that

were not removed by the CXC standard processing. The aspect solution still contains a systematic uncertainty of the order of 1-2 arcseconds. We remove these systematics by applying SIMBAD positions of 3 very bright and identified stars in the field of view. With this technique we are able to reduce any systematic offsets between the 1999 Oct. and the 1999 Nov. observations to less than half a pixel or 0.2 arcsec. All currently available calibration products are normalized to a split grade selection of ASCA grades of 0, 2, 3, 4, and 6. For the data analysis we mainly used FTOOLS 4.2, XSPEC 10.0, and custom software. Errors of the spectral analysis are based on 90% confidence. Errors in fluxes and luminosities are based on the current status of effective area calibration on the ACIS-S3 device, which predicts uncertainties of the order of 10% over the energy range between 0.6 and 8 keV.

For source detection we use the standard 'celldetect' algorithm offered by CXC with a signal to noise threshold set to 10 σ. However since we allow a lower detection limit of 7 counts above background within 0.7" radius, we added a few more fainter sources to the list by hand. The average background level within this selection radius was about 1 count. This corresponds to a sensitivity limit of 3×10^{-15} erg cm^{-2} s^{-1} or a lower limit in luminosity of 6.6×10^{28} erg s^{-1} (for these estimates we applied a 1 keV Raymond-Smith model with the column density determined in section 4). In the second observation this limit is slightly higher because of the shorter exposure, resulting in a limiting luminosity of 1.0×10^{29} erg s^{-1} . Because of the likelihood of source variability we ran source detection on the two single fields of view as well as the merged fields. The sensitivity limit of the latter is 4.0×10^{28} sec. For the search for diffuse emission we are not bound to the source detection radius of 0.7", but applied the detection threshold to a unit area of one arcsec^2, which translates into a sensitivity limit of 2.0×10^{28} erg s^{-1} arcsec^2.

3. WIDE FIELD OBSERVATIONS

Figure 1 shows a 160"x160" area around the Trapezium , the October view in 1a, the November view 1b. This region is relatively free of photons dispersed into first and higher orders by the gratings.

The colors in Figure 1 represent different energy bands. Red was selected for 0.1 to 1.0 keV, green for 1.0 to 1.5 keV, and blue for 1.5 to 10.0 keV. The energy boundaries were chosen to represent typical stellar spectra (Raymond-Smith models around 1 keV) for moderate galactic absorption. In this respect a star that appears red has either a very soft spectrum or appears in the foreground. On the other hand, if a star appears blue it is likely absorbed and has a hard spectrum; while if it appears white, it likely has a hard but less absorbed spectrum.

A comparison of the two star fields shows that the whole field is resolved into point sources. We detected 111 sources within a field of 160"x140". These sources are listed in table 1 with count rates for each of the two observations, as well as the total number of detected counts in the combined (1999 Oct. plus 1999 Nov.) data set. The sources are labelled A-E for the main Trapezium stars and then by numbers and are sorted by RA (2000). So far we identified all but 6 sources in the field and we show the various references in table 1. A more thorough discussion of these identifications will follow in paper II. The central star of the Trapezium is also the brightest X-ray object in the field. Most sources, however, are very faint. Only 7 of the 111 detected sources show X-ray fluxes $> 10^{-12}$ erg cm^{-2} s^{-1} ($> 2 \times 10^{31}$ erg s^{-1}). Many sources in Fig. 1 appear blueish in color. As a guideline, the central star θ^1 Ori C has the assumed column density (see Sec. 4) and appears more white and red in color in Fig. 1.

Clearly these blue sources are significantly more absorbed than θ^1 Ori C, which indicates that they either are intrinsically absorbed or lie deeply embedded in L1641. This is consistent with the earlier observation by Garmire et al. (2000). Sources in the northeastern part of the field appear more affected by this, which may indicate that many of them lie indeed embedded in L1641. There is also an indication that most X-ray sources are confined to within an 0.1 pc radius of the Trapezium, i.e the source density drops considerably to the south and west of the cluster.

A comparison of figures 1a and b show that most of the absorbed blue sources also appear to be the most variable, with flux changes of a factor 5 or more. About 15% of the sources in Table 1 show this behavior. However not all the blue X-ray sources are variable and it is not possible with these two observations to determine a proper variability time scale. Since most of these sources do not vary significantly within the observation intervals of 1999 Oct. and 1999 Nov., we conclude that we observe variability timescales on half a day and longer. Variability on shorter timescales may be possible (see Garmire et al. 2000), but in most cases the statistics per bin do not allow for a conclusive result. The two lower panels in figure 2 (source 78 and 65) show typical light curves obtained from these sources. In some cases we observe slightly enhanced, flare-like activity over 10 to 20 ks. Also a small fraction ($< 5\%$) of the less absorbed sources show variability. In these sources we observe giant flares, in which the X-ray flux changes from the detection limit to about a factor 10 to 30 above within 1 to 3 ks, with decay times of 10 to 20 ks. The second panel in figure 2 (source 80) demonstrates such a behavior.

4. THE RESOLVED ORION TRAPEZIUM

As a subset of the observed star field we focus in the following sections on the Orion Trapezium and its immediate environment. The positions in Table 1 for the five Trapezium stars agree well with the positions found recently by Simon et al. (1999). Figures 1c and 1d show a 30 arcsec blowup from figures 1a and 1b around the Trapezium. Some of the detected sources are too faint to accumulate a broadband spectrum and may not show well in the Figure. We mark some of the sources with circles in the field in which the detected number of counts is the larger of the two observations. Figure 3 shows a contour plot of the merged fields around the Trapezium. The results of the X-ray analysis are summarized in table 2. For the spectral fits as well as flux determinations we used one or, where applicable, two-temperature Raymond-Smith model spectra.

4.1. Diffuse Emission

We searched for diffuse emission within the Trapezium. This is actually very difficult because of the dominance of the point spread function (PSF, from CIAO 1.1 release) of θ^1 Ori C. Because of its proximity to Earth we do not anticipate a contribution from a scattering halo due to interstellar material. From the measured column density in section 4.2 we predict an 0.8% contribution to the surface brightness (Predehl & Schmitt 1995). In order to estimate the fraction of a possible diffuse emission component within the field shown in figure 1c, we removed all detected sources within a radius of 2" of the detected

PSF centroid, except for $\theta^1 Ori$ C, A and E, which are the dominating PSFs, and summed all counts. The count fraction of the sum of $\theta^1 Ori$ A and E to $\theta^1 Ori$ C is 50.4%. We then removed the counts within a 2" radius in $\theta^1 Ori$ C, A and E as well, and compared the remaining fraction to what one would expect from the modelled fractional encircled energy function of a PSF for a point source. A comparison of the measured to the modeled count fraction revealed equivalence within 1.5%, which is within the statistical uncertainties involved. Thus with high confidence we do not detect any diffuse emission above our sensitivity limit.

4.2. *The Early Type Stars $\theta^1 Ori$ A-E: Emission from Stellar Winds*

The measured ACIS/HETGS zeroth-order count rates range from 0.21 cts/s for the brightest component $\theta^1 Ori$ C, to 0.002 cts/s for its faintest member $\theta^1 Ori$ D. The three brightest members, C, E, and A, appear persistently bright with X-ray luminosities (from table 1) between 1.85×10^{32} erg s^{-1} and 2.08×10^{31} erg s^{-1}. Their light curves (figure 2 top, for $\theta^1 Ori$ C) do not show variability. The ACIS spectra required more than one spectral component to give good fits. Here we applied a two-temperature Raymond-Smith model (fixed at solar abundances). The resulting fits are remarkably similar for the three stars, with all three showing a soft component between 0.80 and 0.89 keV and a hard component between 2.18 and 3.15 keV. The flux ratios of hard flux over soft flux in E and A are 0.26 and 0.40, respectively, while in C the same ratio is only 0.07. As a consequence of about 20% photon pileup in the CCD spectra, the results for $\theta^1 Ori$ C are somewhat uncertain. Here we refer to the detailed analysis of high resolution grating spectra from $\theta^1 Ori$ C (Schulz et al. 2000).

An important result of our analysis is the determination of the column density along the line of sight towards the Orion Trapezium. Here we make the assumption that $\theta^1 Ori$ A, C, and E are foreground objects projected onto L1641 and hence are not significantly intrinsically absorbed, such that they are good representatives of the column density towards the Trapezium stars. The measured column densities are very similar in all the sources and the average yields $1.93 \pm 0.29 \times 10^{21}$ cm^{-2}. Given the foregoing assumption, we consider that sources that show significantly higher absorption than this value are either intrinsically absorbed or lie behind the Trapezium, such that they are embedded within L1641.

The X-ray emission from $\theta^1 Ori$ B and D have quite different signatures compared with the other three stars. Their X-ray fluxes and luminosities are an order of magnitude lower and they appear persistent within each observation, with luminosities between 1.94 and 1.51×10^{30} erg s^{-1} for $\theta^1 Ori$ B and 3.12 to 3.22×10^{29} erg s^{-1} for $\theta^1 Ori$ D.

The spectral fit results of $\theta^1 Ori$ B and $\theta^1 Ori$ D are very different as well. $\theta^1 Ori$ B is probably the most peculiar system within the Trapezium since it is a quadruple system (Petr et al. 1998). With a separation of 0.97" from optical observations, we clearly see $\theta^1 Ori$ B as a double star (see figure 3), however with the dominating X-ray emission positioned on component B1. Some emission extends onto component B, however since the flux fraction of the extended emission is less than 5% we can only provide the peak position as a detected source in table 1. The spectral fit clearly rejects two components and the column density could not be constrained during the fit. We then fixed the absorbing column at 1.38×10^{21} cm^{-2}, where the fit

shows a very shallow minimum. To fix this parameter near the value measured for the other Trapezium stars is justified, since $\theta^1 Ori$ B is an identified member of the Trapezium. Independent of the column density we find that the spectral fits do not require a soft component $\theta^1 Ori$ A, C, and E.

$\theta^1 Ori$ D has the lowest observed flux of the five Trapezium stars. The fitted column density is slightly lower than observed in $\theta^1 Ori$ A, C, and E. The spectral fit shows that, in contrast to the other members, no hard component is present. The fit yields a temperature of kT = 0.7 keV. If we compare the flux of this spectrum to the soft flux fraction observed in $\theta^1 Ori$ A, C, and E, we find that it is an order of magnitude lower.

4.3. *Young Stellar Objects and Proplyds*

From the analysis of the of the two observations it is clear that the core of the Orion Trapezium Cluster harbours a large variety of hard, embedded, and variable sources. We detect several faint X-ray sources projected within the Trapezium, as well as in its close vicinity.

The X-ray light curve of source #80 (figure 2) clearly shows a quite powerful X-ray flare in 1999 October, with a rise time of 2 ks and an exponential decay time of 20 ks. During the outburst the source shows an average X-ray luminosity of 2.2 $\times 10^{31}$ erg s^{-1}, with a peak luminosity of 5.5×10^{31} erg s^{-1}. Before the flare as well as throughout the second observation its X-ray luminosity is about a factor 20 lower. We can only accumulate a spectrum during the flare. It shows a very high temperature of 4 keV. This outburst is quite reminiscent of recent observations of hard flares in the Orion region (Yamauchi & Kamimura 1999) as well as the ρ Oph Dark Cloud (Kamata et al. 1997) with *ASCA*. The source is identified within 0.1" with the radio source GMR 25 (Garay et al. 1987) and was also seen at $2.2\mu m$ by Simon et al. (1999). From the *ASCA* observations it remained still uncertain whether class 0 or class I protostars could be the origin of these flares. From the radio variability, Felli et al. 1993 classified the radio emission of this source as non-thermal, which excludes a class 0 object, which should emit thermal radio emission only (Carkner et al. 1998). Since no thermal radio emission has been reported so far, and the persistent X-ray luminosity of this source (1.1×10^{30} erg s^{-1}) is quite strong, we conclude that this flare is associated with a Class II or III T Tauri star.

GMR 3 is another radio source detected near the Trapezium, which coincides within 0.1" with source #78. The light curve in figure 2 shows that it is persistently bright, showing some enhanced X-ray activity at the end of the second observation. This source appears deeply embedded with a column density of up to 2.61×10^{22} cm^{-2}, which is a factor 10 higher than expected for the Trapezium. Its X-ray flux is relatively constant within the first observation, but shows some variability in the second observation. The spectrum can be fit by a similar single temperature spectrum in both observations with temperatures of kT = 1.65 and 1.85 keV, respectively. It shows constant but weak thermal radio emission, which indicates a young object. The star is visible in IR as well as optical and shows strong Hα emission. O'Dell & Wen (1994) identified this object as a proplyd. In a survey of stellar properties of the ONC Hillenbrand derived an age for this star of 1.4×10^5 yr. Given the properties above we conclude that the absorbed X-ray emission is associated with a class II T Tauri star surrounded by a circumstellar disk.

Source #64 is detected at $2.1\mu m$ (McCaughrean & Stauffer

1994). It is also listed in the SIMBAD catalog as [OW94]161-323, although O'Dell & Wen (1994) do not explicitly identify this position with a proplyd. In X-rays it is highly variable, with an X-ray luminosity of 7.7×10^{30} erg s^{-1} in the first, but below the detection threshold of 1.1×10^{29} erg s^{-1} in the second observation. The source is clearly absorbed and hard, however we cannot properly determine a temperature. Source #65 has very similar X-ray properties. It is identified with the thermal radio source GMR 7. Bally et al. (1998) describe this object as an externally illuminated young star-disk system ([OW94]163-317). The light curve of source #65 is shown in figure 2 at the bottom. It does not show much short term varibility, but it appears that the source changes in flux by more than an order of magnitude on timescales of at least one half day.

Sources #58, 70, 72, and 74 were too faint to accumulate significant spectra though they appeared well above the detection threshold at luminosities between 5×10^{29} and 3×10^{30} erg s^{-1} , assuming an absorbed spectrum similar to that determined for source # 78. Source #58 is only identified with an IR position (McCaughrean & Stauffer 1994), the others with thermal radio sources GMR 21, 6, and 17 (Garay et al. 1987), respectively, as well as optical (O'Dell & Wen 1994), and IR (McCaughrean & Stauffer 1994) sources. Except for #58, they appear variable in our two observations, i.e are only detected in one of them, and O'Dell & Wen (1994) identify proplyds within 0.3" of these positions.

In order to emphasize the strong correlation of the X-ray emission in the Trapezium with the optical emission observed with the Hubble Planetary Camera in figure 3 we overlay our X-ray data onto data from Figure 2 in Bally et al. (1998), which is a composite image from narrow band filter observations of N II, Hα, and O I. θ^1Ori B shows emission from both components, with B1 clearly dominating. The overlaid X-ray contours clearly show that many of the proplyds are X-ray sources (e.g., sources 65, 70, 72, 74); although source 64 clearly cannot be associated with 161-322. The overlay also shows that many of the other proplyds in the vicinity do not show X-rays; however, if we lower our threshold to 3σ, we find enhanced X-ray emission coincident with at least two more proplyds.

5. SUMMARY AND DISCUSSION

Our two observations of the Orion Trapezium Cluster in 0th order of the Chandra HETGS with a spatial resolution of 0.5" thoughout almost the entire field of view reveal many new details about the X-ray properties of the Cluster. They allow us to resolve the Trapezium Cluster entirely into point sources, study their variability patterns and perform detailed X-ray spectroscopy. Here we report on the following results:

We resolved all the emission around the Trapezium into point sources, detecting 111 X-ray sources. The cluster shows no diffuse emission above the total (both observations merged) sensitivity limit of 2.0×10^{28} erg s^{-1} per arcsec^2. Besides the five main Trapezium stars we detected six additional X-ray point sources in the close vicinity of the Trapezium. Most sources are faint. Only 12 sources have persistent X-ray luminosities above 10^{31} erg s^{-1} ; four of these are part of the Trapezium and are identified with early type stars. The avarage luminosity of the fainter X-ray sources is around 3×10^{30} erg s^{-1} , in agreement with the result from Garmire et al. (2000) for solar mass PMS stars.

The two observations showed considerable variability on timescales larger than 0.5 days. Fifteen percent of the sources vary by more than a factor 5 in luminosity; the largest excursion

in luminosity was from 1.3×10^{31} erg s^{-1} to 4.1×10^{29} erg s^{-1} . Most of these variable sources appear absorbed with column densities between 1.7×10^{21} cm^{-2} to 1.1×10^{24} cm^{-2} with standard deviations of 5% and 10% respectively. The three bright Trapezium stars display very similar values of line of sight column density, with a mean value of $N_H = 1.93\pm0.29\times10^{21}cm^{-2}$.

The most luminous source is θ^1 Ori C with L$_x = 1.85\pm0.18\times10^{32}$ erg s^{-1} . This is an order of magnitude lower than the estimated luminosity from *ASCA* of 10^{33} erg s^{-1} . If we integrate the luminosities of all sources within the *ASCA* point spread function, however, we get a reasonably consistent result. Stahl et al. (1993) measured a period of 15.4 days in optical and UV data, which was also seen in the *ROSAT* HRI data (Caillault et al. 1994). From the ephemeris given by Stahl et al. we determine phases of 0.68 for our first, and 0.23 for our second observation. From the HRI peak luminosity of given in Caillault et al. we expect luminosites of 2.3×10^{32} erg s^{-1} and 2.0×10^{32} erg s^{-1} , respectively, for our observations. Although the results in Table 1 are slightly lower than these estimates, they are not inconsistent given the various systematic uncertainties.

5.1. *Early Type Stars*

Efforts to model X-ray spectra from stellar winds have been quite modest since the first observations with *Einstein* (Seward et al. 1979). The main reason is that the theory of line radiation-driven stellar winds, which explains successfully the mass loss from a hot luminous star from UV data, could never correctly predict observed X-ray fluxes. Therefore to date no definitive models for the production of X-rays in stellar winds exist. The X-ray emission is now thought to be produced by shocks forming from instabilities within a radiatively driven wind (Lucy & White 1980), where hot blobs plow through rarified cool wind material well into the terminal flow of the wind (Lucy 1982). This model produces X-rays of about 0.5 keV temperature. Hellier et al. (1993) fitted high signal-to-noise PSPC spectra of ζ Pup with detailed NLTE models under the assumption that the X-rays arise from shocks distributed throughout the wind and allowing for recombination in the outer regions of the stellar wind. The best fits predicted two temperatures of 1.6 and 5.0×10^6 K with shock velocities around 500 km s^{-1}.

We performed detailed spectroscopy on the Trapezium stars as well as for most of the nearby X-ray sources. θ^1 Ori A and E are the brightest sources besides C, with persistent X-ray luminosities above 10^{31} erg s^{-1} . None of these sources are observed to be variable by more than 10%. All three sources are identified with massive, very early type stars: θ^1Ori C is a massive ($\sim 25\,M_\odot$) O7V star with a recently discovered low-mass companion (Weigelt et al. 1999); θ^1Ori A is identified with an eclipsing binary of 0.2" separation and a 63.43 day period; θ^1Ori E is a massive early B0.5 type star, and so far no companion has been detected. The main component of θ^1Ori A is not very well determined and speculations range from spectral type B0V to B1V (Lloyd & Strickland 1999). The nature of the companion is similarly unclear and identifications range from a low-mass pre-main sequence star (Strickland & Lloyd 2000) to a B8-AOV type star (Vitrichenko 1999). There are indications that θ^1Ori A is even a triple system (Petr et al. 1998). The spectra of θ^1Ori A, C, and E were fitted with a two-temperature Raymond-Smith spectrum of kT $\sim$ 0.8 keV and kT $\sim$ 2-3 keV. Since these sources are identified with very early type, massive stars we conclude that the X-ray spectra show X-ray emission characteristics of strong stellar winds. Specifically, in the case

of $\theta^1 Ori$ A it is more likely that the X-rays originate from its very early type main component and not from any companion. In fact if the companion is a T Tauri star, its X-ray spectrum may only contribute a small fraction of the observed flux. If it is a late type B-star, we would not expect any X-rays at all (Berghöfer & Schmitt 1994). The spectral fits also agree with the results from previous *ASCA* observations (Corcoran et al. 1994, Cohen et al. 1996) that X-rays from early type stars have two or more temperature components.

The sources θ^1 Ori B and D have luminosities well below 10^{31} erg s^{-1} . The fainter one, θ^1 Ori D, shows only a soft component of 0.7 keV and we may speculate that here the wind lacks the hot component observed in θ^1 Ori A, C, and E, which are of earlier type. The *ROSAT* spectrum of λSco and α Vir, which are of similar spectral type (B1V), show similar luminosities and spectral temperatures. Here we may observe an effect, that with increasing spectral type not only the X-ray luminosity decreases but also the spectrum softens. θ^1 Ori B is brighter, lacks the soft component, and shows a hot component. The second member of θ^1 Ori B, θ^1 Ori B1, whose stellar type is not precisely known, seems to be the dominating source for the observed X-rays. Star B is identified with a spectral type of B3V (Abt et al. 1991), which may already be late enough to have such a weak wind that it cannot produce the X-ray luminosities observed. *ROSAT* observations indicate that in B-stars of later type, the luminosity decreases. Cassinelli et al. (1994) analysed several B-stars of this particular spectral type and found soft X-ray luminosities of the order of 10^{28} erg s^{-1} and lower, which is well below our sensitivity limit. On the other hand, star B1 is thought to be of earlier type (B1) and *ROSAT* observations predict X-ray luminosities of above 10^{30} erg s^{-1} , which we do not observe. It also remains unclear why we observe such hard spectrum.

The spectra of the early type stars in the Trapezium seem unusually hot compared to what stellar wind models currently predict. Four of the five main components, A, B, C, and E, show spectral temperatures between 2.4×10^7 K and 3.7×10^7 K, which is an order of magnitude hotter than current stellar wind models predict. In the case of θ^1 Ori C, Schulz et al. (2000) recently determined a temperature range of 0.5 to 6.1×10^7 K from X-ray emission lines. These temperatures were deduced from H-like ion species up to S XVI and Fe XXV, which rules out a significant inverse Compton continuum as suggested by Chen & White (1991). Babel & Montmerle (1997a) presented the hypothesis that in the case of θ^1 Ori C a dipolar magnetic field is embedded in the radiation-driven wind and X-rays are produced by a magnetically confined wind shock. In the case of the hot A0p star IQ Aur, Babel & Montmerle (1997b) modelled temperatures up to 9×10^6 K by including the effects of magnetic confinement. If in addition substantial stellar rotation was included, temperatures could be as high as 3×10^7 K. Therefore it seems compelling to include magnetic field effects as well as centrifugal forces into stellar wind models for these hot stars. The fact that such high temperatures are present in θ^1 Ori A, B, and E, as well as in τSco (Cohen et al. 1997), also shows that these effects may be more common in early type stars.

5.2. *YSOs*

Although it is now widely accepted that X-ray emission from young stars emerges from hot stellar coronae heated via a stellar dynamo, the underlying physics of this mechanism is still poorly understood. High levels of magnetic activity in connection with rotation, accretion, and/or outflows may play a key role (see Feigelson & Montmerle 1999 for a review). Recent imaging observations showed that the X-rays of most T Tauri stars vary on time scales of days and a substantial number of stars display high amplitude flares with time scales of hours. X-ray spectra show more than one temperature and are usually modelled with soft spectral components of $2-5 \times 10^6$ K and some hard components during flares of up to 3×10^7 K. Montmerle et al. (2000) recently modelled the X-ray emission from a giant flare with a peak temperature of 7×10^7 K in YLW 15 observed with *ASCA* (Tsuboi et al. 2000) with strong magnetic shearing and reconnection between the central star and the accretion disk. In the case of WL 6 (Kamata et al. (1997) the X-ray flaring is rotationally modulated (see also Stelzer et al. 1999). Montmerle et al. (2000) inferred a mass-rotation relation, in which higher mass stars are fast rotators and giant hard flares are generated through strong star-disk magnetic interactions, while lower mass stars are slower and and their X-ray emission is solely of stellar origin.

The vicinity of the Orion Trapezium harbours a large variety of YSOs. Most notable are the large number of proplyds detected with the Hubble Space Telescope (O'Dell et al. 1993). We detected 8 faint X-ray sources, where six sources are identified with radio objects, five sources with proplyds in the vicinity of θ^1 Ori C (i.e. proplyds 163-317, 166-316, 167-317, 168-328, and 171-334). One source is identified with a YSO in the the IR only. These X-ray sources show luminosity variations between a factor 3 and 10, and have spectra indicating that they are heavily absorbed. The X-ray emission, together with optical, IR and radio surveys (Bally et al. 1998, McCaughrean and Stauffer 1994, Felli et al. 1993) indicate that these sources are embedded Class I, Class II, or Class III protostars. We do not believe that the X-rays are generated through induced shocks by the wind θ^1 Ori C. First, the flux of these sources varies by large factors which we would not expect under constant illumination unless the density structure in the wind shock at the proplyds changes similarly. That would imply similar brightness variations in the optical, but no such variations have been reported so far. On the other hand, in source #78 we see variability timescales of the order of 10 min to 2 hours (figure 2). From this we deduce an upper limit of the size of the emitting region of the order of 1.0 - 12 AU, which is too small compared to size of the proplyds ($\sim$ 500 AU, Bally et al. 1998). Second, the spectra we analysed are intrinsically absorbed. Thus the emission likely originates from deep inside the dusty disks, rather than from the wind shock region.

In the context of recent observations of hard X-ray emission from YSOs, these results are quite remarkable; the light curves indicate that only one of the sources actually displays large flaring activity, and the others are persistent in flux with some minor activity. Very large flux variations occur only on time scales longer than 12 h. The spectra, however, indicate extremely high temperatures at quite modest luminosities, from which we conclude that the X-ray emission may not be related to star-disk magnetic interactions in connection with rapid rotation as proposed by Montmerle et al. (2000). The observed X-ray behavior of these proplyds seem more related to recent *ASCA* observations of SU Aurigae (Skinner & Walter 1998), which has been identified with a type G2 CTTS and where it was suggested that the X-ray emission arises from a magnetically confined stellar plasma. In this respect long term X-ray

observations of these proplyds will not only enhance the significance of these hot spectra but also allow a search for rotational modulations and lead to better understanding of the magnetic properties and their role in the evolution of these protostars.

The authors thank John Bally for generously providing us

REFERENCES

Abt H.A., Wang R., and Cardona O., 1991, ApJ 367, 155

Ali, B., & Depoy, D. L. 1995, AJ 109, 709

Babel J., & Montmerle T., 1997a, ApJ 485, L29

Babel J., & Montmerle T., 1997b, A&A 323, 121

Bally J., Sutherland R.S., Devine D., and Johnstone D., 1998, AJ 116, 293

Berghöfer T.W., and Schmitt J.H.M.M., 1994, A&A 292, L5

Carkner L., Kozak J.A., and Feigelson E.D., 1998, AJ 116, 1933

Casinelli J.P., Waldron W.L., Sanders W.T., Harnden F.R., Rosner R., and Vaiana G.S., 1981, ApJ 250, 677

Casinelli J.P., Cohen D.H., MacFarlane J.J., Sanders W.T., and Welsh B.Y., 1994, ApJ 421, 705

Chen W., & White R.L., 1991, ApJ 366, 512

Cohen D.H., Cassinelli J.P., and Waldron W.L., 1997, ApJ 488, 397

Corcoran M.F., Waldran W.L., MacFarlane J.J., et al., 1994, ApJ 436, L95

Feigelson E.D., Casanova S., Montmerle T., Guibert J., 1993 ApJ 416, 623

Feigelson E.D., and Montmerle T., 1999, ARA&A 37, 363

Felli M., Taylor G.B., Catarzi M., Churchwell E., and Kurtz S., 1993, A&ASuppl. 101, 127

Gagné M., Caillault J.-P., and Stauffer J.R., 1995, ApJ 445, 280

Garay G., Moran J.M., and Reid M.J., 1987, ApJ 314, 535

Garmire G., Feigelson E.D., Broos P., Hillenbrand L., Pravdo S.H., Townsley L., and Tsuboi Y., 2000, AJ in press

Gaume, R. A., Wilson, T. L., Vrba, F. J.,Johnston, K. J., & Schmid-Burgk, J. 1998, ApJ 493, 940

Geier S., Wendker H.J., and Wisotzki L., 1995, A&A 299, 39

Giaconni R., Murray S., Gursky H., Kellogg E., Scgreier E., and Tananbaum H., 1972, ApJ 178, 281

Hayward T.L., Houck J.R., and Miles J.W., 1994, ApJ 433, 157

Hillier D.J., Kudritzki R.P., Pauldrach A.W., Baade D., Casinelli J.P., Puls J., and Schmitt J.H.M.M., 1993, A&A 276, 117

Hillenbrand L.A., 1997, AJ 113, 1733

Hyland, A. R., Allen, D. A., Barnes, P. J., & Ward, M. J. 1984, MNRAS 206, 465H

Jorgensen, U. G., & Westerlund, B. E. 1988, A&ASuppl., 72, 193

Kamata Y., Koyama K., Tsuboi Y., and Yamauchi S., 1997, PASJ 69, 461

Kastner J.H., Zuckerman B., Weintraub D.A., and Forveille T., 1997, Science 277, 67

Ku W.H.-M., and Chanan G.A., 1979, ApJ 234, L59

Ku W.H.-M., Righini-Cohen G., and Simon M., 1982, Science 215, 61

Lloyd C., and Strickland D.J., 1999, IBVS No. 4809

Lucy L.B., and White R.L., 1980, ApJ 241, 300

Markert T.H., Canizares C.R., Dewey D., McGuirck M., Pak C., and Schattenburg M.L., 1994, Proc SPIE 2280, 168

McCaughrean M.J., and Stauffer J.R., 1994, AJ 108, 1382

Munch, G. 1977, ApJ 212, L77

Montmerle T., Grosso N., Tsuboi Y., and Koyama K., 2000, ApJ 532, 1097

O'Dell C.R., and Wen Z., 1994, ApJ 436, 194

Petr M.G., Coudé du Foresto V., Beckwith S.V.W., Richichi A., and McCaughrean M.J., 1986, ApJ 500, 825

Predehl P., and Schmitt J.H.M.M., 1995, A&A 293, 889

Prigozhin G., Kissell S., Bautz M., Grant C., LaMarr B., Foster R., and Ricker G., 2000, Proc. SPIE 4012, in press

Prosser, C. F., Stauffer, J. R., Hartmann, L., Soderblom, D. R., Jones, B, F., Werner, M. W., McCaughrean, M. J. 1994, ApJ 421, 517

Rieke, G. H., Low, F. J., & Kleinmann, D. E. 1973, ApJ 186, L7

Schulz N.S., Canizares C.R., Huenemoerder D., and Lee J., 2000, ApJLetters, in press

Simon M., Close L.M., and Beck T., 1999, ApJ 117, 1375

Skinner S.L. and Walter F.M., 1998, in "Cool Stars, Stellar Systems, and the Sun", eds. R.A. Donahue and J.A. Bookbinder, ASP Conference Series, Vol. 154, p. 1787

Stahl O., Wolf B., Gäng T., Gummersbach C., Kaufer A., Kovács J., Mandel H., Szeifert T., 1993, A&A 274, L29

Stelzer B., Neuhäuser R., Casanova S., and Montmerle T., 1999, A&A 344, 154

Strickland D.J., and Lloyd C., 2000, The Observatory 200, in press

Trumpler R.J., 1931, PASP 42, 255

Tsuboi Y., Imanishi K., Koyama K., Grosso N., and Montmerle T., 2000, ApJ 532, 1089

Vitrichenko E.A., 1999, Astr. Lett. 25, 179

Weigelt G., Balega Y., Preibisch T., Schertl D., Schöller M., and Zinnecker H., 1999, A&A 347, L15

Weisskopf M.C., O'Dell S.L., and van Speybroeck L.P. 1996, Proc. SPIE, 2805, 2

Yamauchi S., Koyama K., Sakano M., and Okada K., 1996, PASJ 48, 719

Yamauchi S., and Kamimura R., 1999, "Star Formation 1999", sf99.proc, 308Y

TABLE 1
SOURCE POSITIONS, COUNT RATES AND IDENTIFICATIONS.

#	α, δ(2000) $5^h 35^m, -5°$	total cts (Oct/Nov)	Oct. 99 10^{-3} cts/s	Nov. 99 10^{-3} cts/s	ID
A	$15^s.82, 23'14".19$	3014	35.65	39.02	θ^1 Ori A
B	$16^s.07, 23'06".99$	263	3.34	3.03	θ^1 Ori B
C	$16^s.46, 23'22".89$	16640	205.64	201.31	θ^1 Ori C
D	$17^s.25, 23'16".53$	152	1.77	2.01	θ^1 Ori D
E	$15^s.77, 23'09".86$	5372	61.50	72.84	θ^1 Ori E
6	$11^s.73, 23'40".50$	37	0.34	0.64	[H97b] 9008,[PSH94] 8
7	$12^s.29, 23'48".06$	490	4.16	8.97	Parenago 1825
8	$12^s.35, 22'41".34$	28	0.10	0.73	[AD95] 2736
9	$12^s.41, 23'51".36$	41	0.66	0.26	...
10	$12^s.58, 23'01".96$	47	0.52	0.67	[PSH94] 18
11	$12^s.61, 23'44".19$	51	0.60	0.67	Parenago 1807
12	$12^s.97, 23'54".76$	72	0.62	1.31	[AD95] 3132
13	$12^s.99, 23'30".28$	14	0.14	0.22	[PSH94] 44,[JW88] 412
14	$13^s.22, 22'55".03$	44	0.30	0.93	[AD95] 2717
15	$13^s.31, 22'39".13$	14	0.16	0.19	[GWV98] 053246.204-052432.86
16	$13^s.45, 23'40".29$	171	1.01	3.83	[AD95] 3141
17	$13^s.54, 23'30".98$	62	0.72	0.83	[AD95] 3255
18	$13^s.59, 23'55".40$	81	0.52	1.76	[AD95] 3132
19	$14^s.06, 23'38".48$	37	0.36	0.61	Parenago 1823
20	$14^s.08, 22'22".10$	65	0.94	0.57	[M77] HH08, [S99] 24
21	$14^s.08, 22'36".43$	67	0.52	1.31	[GWV98] 053246.628-052429.82
22	$14^s.29, 23'04".17$	61	0.68	0.86	[MS94] 3, [S99] 27
23	$14^s.27, 24'24".73$	26	0.52	-	Parenago 1826,V V1328 Ori
24	$14^s.32, 23'08".31$	342	2.01	7.70	[H97b] 9061, [S99] 28
25	$14^s.36, 22'32".66$	120	1.49	1.44	[S99] 32
26	$14^s.36, 22'54".02$	38	0.34	0.67	Parenago 1842
27	$14^s.37, 23'33".13$	122	1.13	2.08	Parenago 1843
28	$14^s.40, 22'36".48$	29	0.28	0.48	[JGS92] 2
29	$14^s.50, 22'38".66$	103	1.41	1.02	[RLK73] IRc4 (?)
30	$14^s.55, 23'16".01$	313	0.76	8.78	[MS94] 13, [S99] 49
31	$14^s.57, 24'07".93$	22	0.34	0.16	...
32	$14^s.65, 22'33".67$	310	4.32	2.97	[S99] 38
33	$14^s.67, 23'01".75$	253	4.64	0.64	[S99] 37
34	$14^s.69, 22'49".60$	25	0.28	0.35	[MS94] 11, [S99] 41
35	$14^s.72, 23'22".83$	59	0.60	0.93	[S99] 69
36	$14^s.73, 22'29".70$	809	14.78	2.11	[S99] 46
37	$14^s.80, 24'07".13$	15	0.22	0.13	[AD95] 2626
38	$14^s.83, 23'46".47$	40	0.44	0.57	Parenago 1845,[MS94] 21,[JW88] 464
39	$14^s.87, 22'31".44$	27	0.40	0.22	[S99] 53
40	$14^s.91, 22'39".14$	1090	17.33	6.99	[S99] 56
41	$14^s.89, 22'25".39$	140	1.51	2.04	[S99] 78
42	$14^s.92, 24'12".83$	42	0.48	0.57	[H97b] 9080,[PSH94] 80
43	$14^s.95, 23'39".26$	170	2.13	2.01	Parenago 1844
44	$15^s.09, 22'31".52$	39	0.54	0.38	[H97b] 9086,[PSH94] 86, [S99] 53
45	$15^s.16, 22'17".40$	138	-	4.41	[GWV98] 053247.641-052410.31
46	$15^s.19, 22'24".04$	96	1.01	1.44	[S99] 67, [HAB84] 63
47	$15^s.19, 22'54".12$	69	0.92	0.73	Parenago 1841
48	$15^s.26, 22'56".83$	897	10.60	11.62	Parenago 1862,V V348 Ori
49	$15^s.34, 22'25".32$	37	0.30	0.70	[H97b] 9096, [PSH94] 96
50	$15^s.34, 22'15".47$	365	-	11.66	Parenago 1838
51	$15^s.38, 23'33".57$	56	0.66	0.73	[MS94] 29
52	$15^s.44, 23'45".46$	50	0.76	0.38	[S99] 77, [OW94] 154-346
53	$15^s.49, 22'48".53$	57	0.82	0.51	[S99] 81
54	$15^s.60, 24'03".06$	54	0.70	0.61	[AD95] 3125
55	$15^s.63, 22'56".44$	1996	26.26	21.59	Parenago 1862,V V348 Ori
56	$15^s.68, 23'39".15$	108	0.80	2.17	[MS94] 37, [S99] 87

TABLE 1
SOURCE POSITIONS, COUNT RATES AND IDENTIFICATIONS.

#	α, δ(2000) $5^h35^m,-5°$	total cts (Oct/Nov)	Oct. 99 10^{-3} cts/s	Nov. 99 10^{-3} cts/s	ID
57	$15^s.76, 23'38".40$	44	0.12	1.21	[MS94] 41, [S99] 90
58	$15^s.82, 23'11".94$	52	0.62	0.67	[S99] 93
59	$15^s.84, 22'45".92$	39	0.36	0.67	Parenago 1860
60	$15^s.97, 23'49".70$	751	6.09	14.21	[S99] 104
61	$16^s.07, 23'53".45$	73	0.76	1.12	Parenago 1870, V AC Ori
62	$16^s.08, 24'11".61$	20	0.30	0.16	[AD95] 3123
63	$16^s.07, 22'54".16$	44	0.58	0.48	[MS94] 55, [S99] 114
64	$16^s.10, 23'23".11$	310	5.07	1.76	[OW94] 161-323, [S99] 113
65	$16^s.29, 23'16".50$	215	3.22	1.69	[BSD98] 6,[JW88] 512,[MS94] 63
66	$16^s.37, 24'03".33$	337	4.28	3.90	...
67	$16^s.49, 22'56".30$	21	0.14	0.45	[MS94] 69, [S99] 137
68	$16^s.49, 22'35".24$	21	0.16	0.42	[S99] 138, H97b] 519a
69	$16^s.58, 24'06".11$	119	0.88	2.40	V V1279 Ori, Parenago 1869
70	$16^s.61, 23'16".04$	104	1.19	1.41	[BSD98] 7,[OW94] 166-316,[MS94] 70
71	$16^s.74, 22'31".10$	52	0.42	0.99	[H97b] 9151,[OW94] 167-231, [S99] 145
72	$16^s.74, 23'16".36$	100	1.27	1.15	θ^1 Ori G,Parenago 1890
73	$16^s.76, 24'04".32$	604	7.84	6.71	[H97b] 526b,[PSH94] 150
74	$16^s.77, 23'28".03$	45	0.40	0.80	[BSD98] 5,[MS94] 74, [S99] 144
75	$16^s.88, 22'22".35$	113	1.41	1.34	[S99] 153
76	$16^s.00, 22'32".95$	413	5.15	4.92	[S99] 103
77	$17^s.06, 23'39".74$	66	0.76	0.89	[S99] 160, [AD95] 3144
78	$17^s.06, 23'34".09$	779	7.80	12.36	Parenago 1893
79	$17^s.38, 24'00".24$	48	0.50	0.73	[AD95] 3130
80	$17^s.46, 23'21".08$	881	17.01	0.83	[H97b] 9180,[MS94] 93, [S99] 175
81	$17^s.55, 22'56".73$	58	0.38	1.25	[H97b] 553a,[PSH94] 185
82	$17^s.77, 23'42".63$	89	0.86	1.47	[S99] 192, [H97b] 9195,[PSH94] 195,[MS94] 99
83	$17^s.81, 23'15".70$	18	0.10	0.42	[OW94] 178-316S, [S99] 195
84	$17^s.87, 23'02".99$	72	0.44	1.60	[H97b] 9201,[PSH94] 201,[MS94] 103
85	$17^s.94, 22'45".42$	4222	29.78	87.02	[AD95] 3168
86	$17^s.96, 23'35".50$	40	0.60	0.32	[MS94] 105
87	$18^s.03, 24'03".21$	65	0.92	0.61	[H97b] 9210,[PSH94] 210
88	$18^s.05, 24'01".07$	56	0.68	0.70	...
89	$18^s.19, 23'35".95$	165	2.57	1.15	[AD95] 3271, [OW94] 182-336
90	$18^s.32, 24'04".95$	39	0.50	0.45	V V1336 Ori
91	$18^s.36, 22'37".38$	1135	13.73	14.21	V V1229 Ori,Parenago 1925
92	$18^s.66, 23'13".90$	150	2.17	1.31	[HHM94]12
93	$18^s.69, 22'56".82$	155	1.69	2.24	[H97b] 598a,[PSH94] 235
94	$18^s.95, 22'18".52$	40	-	1.28	[S99] 204
95	$19^s.06, 23'49".75$	30	0.40	0.32	V V1337 Ori
96	$19^s.11, 23'27".02$	25	0.14	0.57	[S99] 235
97	$19^s.20, 22'50".63$	828	1.61	23.85	[H97b] 9250,[MS94] 123,[PSH94] 250
98	$19^s.34, 23'40".56$	14	0.20	0.13	...
99	$19^s.59, 23'57".32$	74	0.72	1.21	[AD95] 2647
100	$19^s.79, 22'21".55$	233	4.58	0.10	...
101	$20^s.17, 23'08".59$	111	0.40	2.91	[H97b] 3075, [AD95] 3270
102	$20^s.45, 23'29".84$	152	1.55	2.36	[H97b] 648b, [PSH94] 62, [AD95] 3151
103	$20^s.53, 24'20".86$	18	0.36	-	[AD95] 3306
104	$20^s.66, 23'53".09$	60	0.72	0.77	[AD95] 3135
105	$20^s.89, 22'34".32$	19	0.18	0.32	[S99] 247
106	$20^s.90, 23'21".83$	191	0.46	5.36	[H97b] 9271
107	$21^s.01, 23'55".59$	24	0.08	0.64	[H97b] 9272, [PSH94] 72
108	$21^s.03, 23'48".00$	1947	17.43	34.20	[H97b] 9287, [PSH94] 78
109	$21^s.22, 22'59".42$	27	0.22	0.51	[AD95] 2720, [H97b] 9280, [PSH94] 280
110	$21^s.31, 24'11".47$	28	0.30	0.42	V V1231 Ori
111	$21^s.35, 23'45".36$	314	5.65	0.96	[PSH94] 279

[AD95] = Ali & Depoy 1995; [H97] = Hildebrand 1997; [JW88] = Jorgensen & Westerlund 1988; [GWV98] = Gaume et al. 1998; [M77] = Munch 1977; [RLK73] = Rieke, Low, & Kleinmann 1973; [HAB84] = Hyland et al. 1984; [OW94] = O'Dell & Wen 1994; [BSD98] = Bally et al. 1998; [HHM94] = Hayward, Houck, & Miles 1994; [MS94] = McCaughrean & Stauffer 1994; [PSH94] = Prosser et al. 1994; [S99] = Simon, Close, & Beck 1999

SCHULZ et al.

TABLE 1
SPECTRAL PARAMETERS FOR IDENTIFIED TRAPEZIUM SOURCES.

src#	$N_H^{(1)}$	kT_1 keV	kT_2 keV	$f_x^{(2)}$	$L_x^{(3)}$	dof	χ^2
A	2.19±0.04	0.87±0.02	2.18±0.12	1.25±0.03	2.08±0.07	314	0.78
	1.49±0.02	0.85±0.04	2.37±0.17	1.26±0.05	2.35±0.11	314	0.62
B	1.38		3.16±0.58	0.12±0.01	0.19±0.02	57	0.48
	1.38		2.04±0.42	0.09±0.01	0.15±0.02	57	0.36
C$^{(4)}$	1.83±0.16	0.83±0.02	3.15±0.27	12.50±0.13	18.52±1.80	312	1.32
	2.03±0.24	0.80±0.03	3.20±0.37	11.59±0.19	17.32±2.31	312	1.07
D	1.65	0.76±0.08		0.05±0.01	0.03±0.01	182	0.16
	1.65±0.05	0.67±0.07		0.04±0.01	0.03±0.01	182	0.11
E	1.97±0.03	0.89±0.02	3.13±0.15	2.58±0.05	4.46±0.12	319	0.90
	2.09±0.03	0.85±0.03	2.50±0.12	2.51±0.07	4.35±0.16	319	0.89
64	5.87±0.19		32.3 ±61.7	0.28±0.02	0.42±0.03	130	0.51
	5.87			0.06±0.01	0.09±0.02		
65	6.05±2.35		31.8 ±41.5	0.13±0.01	0.20±0.01	65	0.59
	6.05			0.02±0.01	0.03±0.01		
78	23.6± 3.4		1.65±0.17	0.34±0.02	1.93±0.37	105	0.60
	26.1± 5.3		1.85±0.18	0.47±0.03	2.37±0.42	105	0.55
80	3.34±0.05		4.28±0.44	0.75±0.02	1.25±0.06	182	0.81
	3.34			0.04±0.01	0.11±0.02		

[1] in units of $10^{21} cm^{-2}$

[2] in units of 10^{-12} erg cm^{-2} s^{-1}

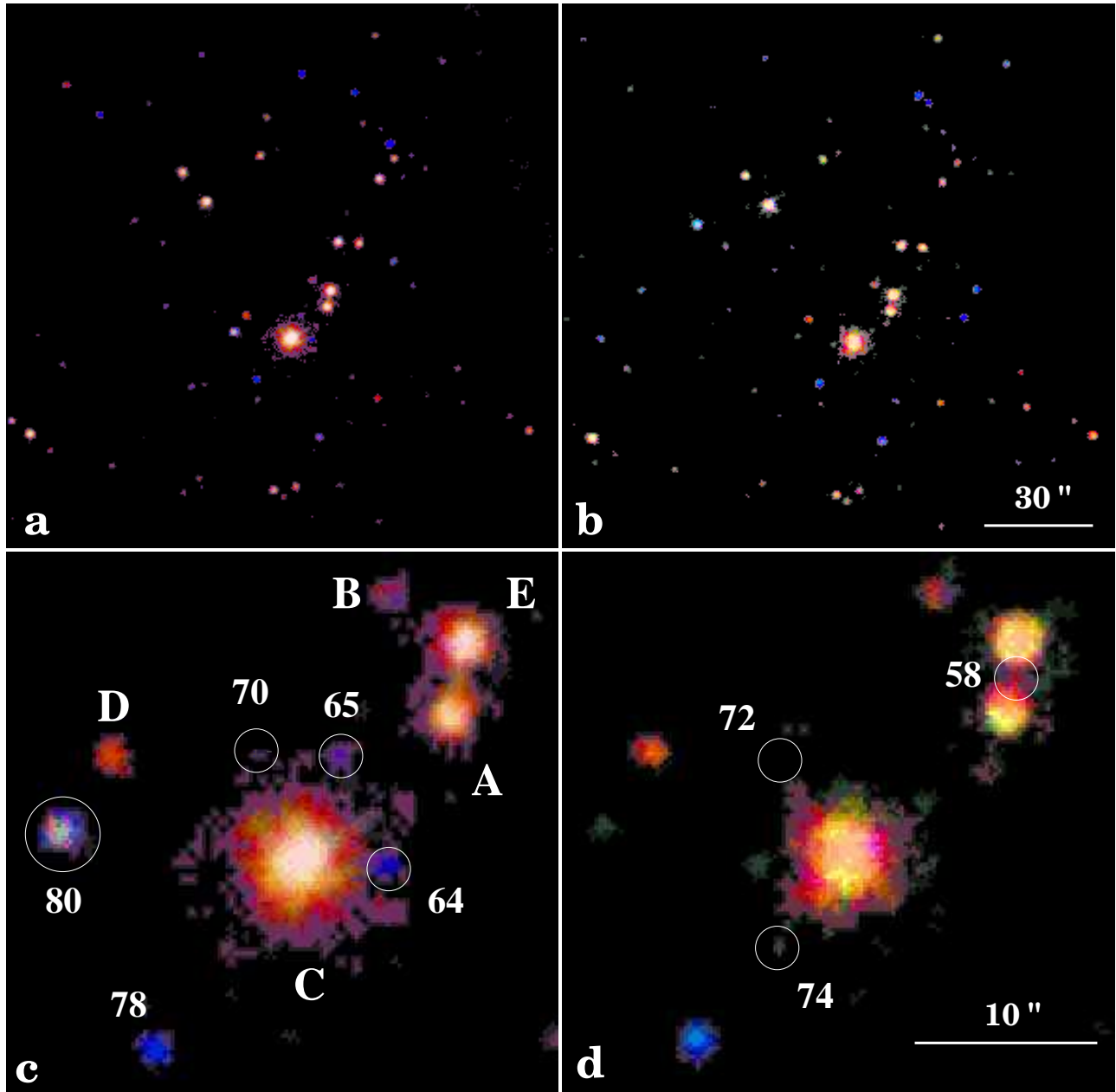[3] in units of 10^{31} erg s^{-1}

[4] spectra affected by approx. 20% pileup

FIG. 1.— X-ray Variability in the Orion Trapezium. (a) and (b) show color coded images of a 160"x160" field around the Trapezium, which are 3 weeks apart. (c) and (d) show the same for a close-up on the Trapezium. The circles indicate the positions of detected sources in the frame where they are brightest.
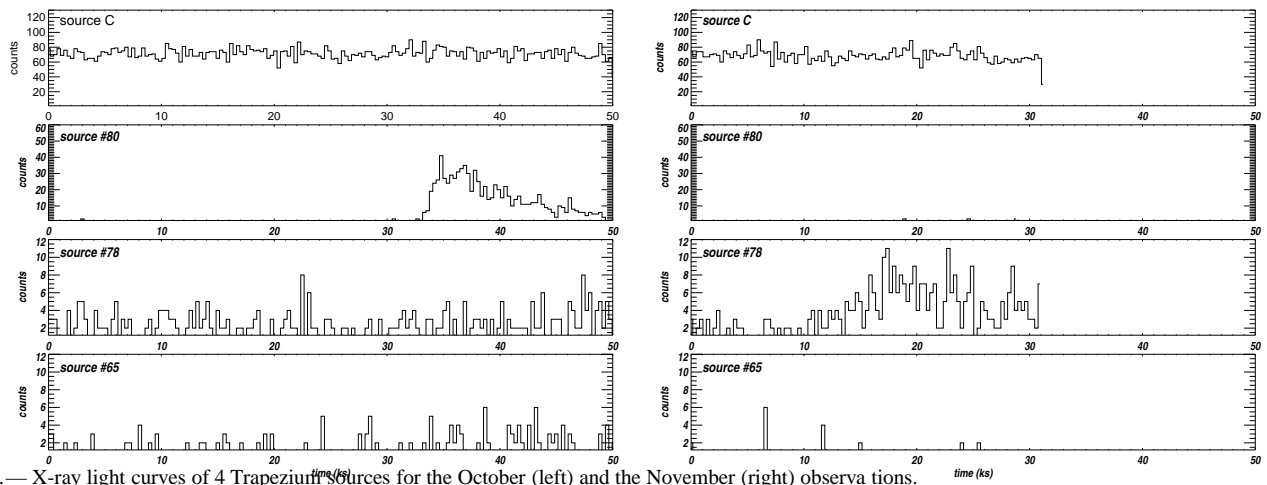
SCHULZ et al.

FIG. 2.— X-ray light curves of 4 Trapezium sources for the October (left) and the November (right) observa tions.

FIG. 3.— X-ray contours of the merged Chanda events overlaid onto an optical HST PC observation (from Bally et al. 1998). The field of view is 30"x30" and the contours represent total counts. The lowest contour represents a flux at about the detection threshold.